Science of the Total Environment 753 (2021) 141985

Contents lists available at ScienceDirect

Science of the Total Environment

journal homepage: www.elsevier.com/locate/scitotenv

Sedimentary DNA record of eukaryotic algal and cyanobacterial communities in a shallow Lake driven by human activities and climate change

Hanxiao Zhang [a,b], Shouliang Huo [a,*], Kevin M. Yeager [c], Fengchang Wu [a]

[a] State Key Laboratory of Environmental Criteria and Risk Assessment, Chinese Research Academy of Environmental Science, Beijing 100012, China,
[b] College of Water Sciences, Beijing Normal University, Beijing 100874, China
[c] Department Earth and Environmental Sciences, University of Kentucky, Lexington, KY 40506, USA.

HIGHLIGHTS

- The temporal dynamic of eukaryotic algae and cyanobacterial community is revealed by sedimentary DNA.
- Nutrient enrichment, hydrological conditions and climate warming are the key controls on the lake ecosystem.
- Generalized additives models are applied to quantify the effects of human activities and climate change.

GRAPHICAL ABSTRACT

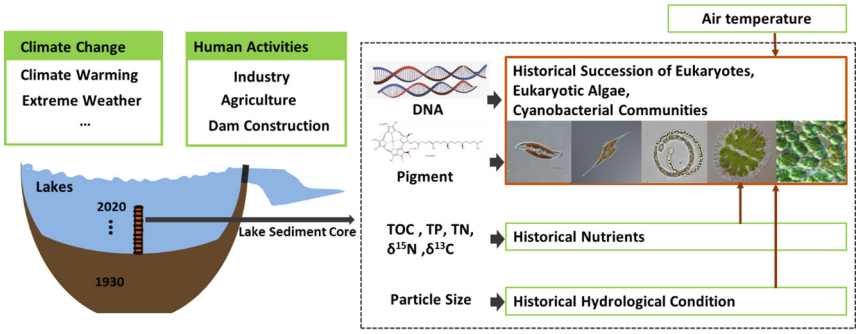

ARTICLE INFO

Article history:
Received 27 February 2020
Received in revised form 11 August 2020
Accepted 24 August 2020
Available online 27 August 2020

Editor: Ouyang Wei

Keywords:
Climate change
Cyanobacterial
Eukaryotic algae
Eutrophication
Sedimentary DNA

ABSTRACT

Global freshwater lakes are changing due to human activities and climate change. Unfortunately, sufficient long-term monitoring is lacking for most lakes. However, lake sedimentary archives can extend the instrumental record and reveal historical environmental trends. In particular, sedimentary DNA analysis of lacustrine sediment cores can aid the reconstruction of past trends in eukaryotic algal and cyanobacterial communities, as was conducted in this study for Lake Chaohu in China. The results presented here indicate that the construction of the Chaohu Dam in 1963 is associated with decreased richness of eukaryotic algal and cyanobacterial communities. Several groups, including the eukaryotic algal taxa, *Chlorophyceae*, and cyanobacterial groups like *Dolichospermum*, *Microcystis*, *Planktothricoides*, *Cyanobium*, *Pseudanabaena*, and *Synechococcus*, increased in abundance following inferred historical nutrient enrichment. Nutrient concentrations and hydrologic conditions were further implicated as the dominant controls on communities based on Random Forest and generalized additive modeling statistical analyses. In particular, significant increases in lake hydraulic residence times after the construction of the Chaohu Dam were significantly associated with altered biological community structures. Further, phosphorus enrichment was positively associated with increased richness and diversity of these communities following the 1980s. In addition, effects from increased atmospheric temperatures on eukaryotic algal and cyanobacterial communities were apparent. Here, high-throughput sequencing analysis of sedimentary DNA allowed the inference of long-term biodiversity dynamics of Lake Chaohu. These results underscore the important impacts of anthropogenic activities and climate change on aquatic ecosystems at the decadal scale.

* Corresponding author.
E-mail address: huosl@craes.org.cn (S. Huo).

https://doi.org/10.1016/j.scitotenv.2020.141985
0048-9697/

1. Introduction

Human activities and climate change are widely recognized as the primary stressors of lake ecosystems (Blois et al., 2013; Capo et al., 2017; O'Beirne et al., 2017). Increasing eutrophication and changes in hydrodynamic conditions caused by the construction of dams are the main human activities responsible for changing the dynamics of lacustrine biological communities (Karlsson et al., 2016; Zeng et al., 2018). These factors may influence the diversity and structure of lacustrine biological communities independently or synergistically over multiple time scales, causing negative effects on aquatic food webs and ecosystem functioning (e.g., Smol et al., 2005; Caron and Hutchins, 2013; Capo et al., 2017). Eukaryotic algae are key components of aquatic ecosystems and play important ecological roles as primary producers (O'Beirne et al., 2017). Recent research has investigated the relative impacts of climate warming and various human activities on lake algal communities, leading to the understanding that these two factors interact either synergistically or antagonistically to alter communities (e.g., Blois et al., 2013; Michalak et al., 2016; Capo et al., 2017). In addition, cyanobacterial blooms pose serious threats to the water quality of lakes, due to their production of high toxin concentrations that poison aquatic animals and limit human use of freshwater resources (Kosten et al., 2012; Yang et al., 2016; Tse et al., 2018). An analysis of 143 lakes along a global latitudinal transect indicated that the synergistic effects of increasing nutrient concentrations and warming climate help drive the proliferation of Cyanobacteria, leading to their dominance in many shallow lakes (Kosten et al., 2012). By improving understanding of historical trends in lake conditions and ecology, policy makers and environmental managers can more effectively respond to environmental changes and proactively avoid or mitigate undesirable ecological consequences. However, long-term monitoring data for both lacustrine biological communities and environmental conditions are scarce for most global lakes (Rigosi et al., 2014).

Lake sediments can help extend historical records from instrument-derived measurements and provide long-term records of environmental changes in addition to the associated changes in biological community compositions and structures via physico-chemical, fossil, and biomolecular proxy analysis within sediment archives, as described previously (Savichtcheva et al., 2015; Chen et al., 2019). The emergence of DNA-based ecological analyses of lacustrine sediment communities has complemented classical paleolimnology proxies and expanded the range of organisms that are detectable in lake sediments (Domaizon et al., 2017; Ficetola et al., 2018; Huo et al., 2020), including those lacking observable morphological or diagnostic features due to preservation issues (Savichtcheva et al., 2015; Domaizon et al., 2017). Nevertheless, the stability of DNA in environments over time represents a potential limitation of its use in paleo-environmental reconstructions. The stability of DNA can decrease over time due to the biotic degradation and abiotic decay of DNA that leads to fragmentation and potential differential taxonomic preservation of DNA due to lake conditions and the sourcing taxa (Barnes et al., 2014; Capo et al., 2016). However, aquatic sedimentary environments have been shown to be rich in DNA, with preservation favored by cold, anoxic conditions. Indeed, the exemplary preservation of sediment DNA and the application of high-throughput sequencing to analyze sedimentary DNA has resulted in successful lacustrine paleo-ecological investigations (Capo et al., 2017; Ficetola et al., 2018; Tse et al., 2018; Chen et al., 2019).

Here, we applied high-throughput DNA sequencing to samples of a sediment core collected from the eutrophied Lake Chaohu in southeastern China. The hydrodynamics of Lake Chaohu considerably changed after a dam was constructed on the Yuxi River in 1963 (Zan et al., 2012). We hypothesized that the hydrographic changes associated with dam construction shifted the composition and structure of eukaryotic algal and cyanobacterial communities within the lake. Moreover, increased urban populations, industrial development, and land-use patterns in the basin have been associated with the conversion of agricultural land to urban and industrial use lands in recent decades (Zan et al., 2012). Consequently, we further hypothesized that effects from nutrient enrichment and climate change have driven the temporal dynamics of eukaryotic algal and cyanobacterial communities within the lake. By applying meta-barcoding approaches to sedimentary DNA recovered from the cores, the objectives of this study were to (1) reconstruct temporal changes in the composition, diversity, and structure of eukaryotic algal and cyanobacterial communities in the lake; (2) identify the relative importance of variation in historical environmental conditions, including nutrient concentrations, hydrologic changes, and warmer temperatures, in determining the past trajectories of eukaryotic algal and cyanobacterial communities; and (3) quantify the contributions of nutrient concentrations, hydrologic changes, and warmer temperatures to changes in eukaryotic algal and cyanobacterial communities over time within Lake Chaohu.

2. Materials and methods

2.1. Study areas and sediment sampling

Lake Chaohu (117°16′–117°51′ E, 31°25′–31°43′ N; Fig. 1) is one of the five largest freshwater lakes in China and is located in eastern China between the Huaihe River watershed and the Yangtze River Delta. The lake averages 3.0 m water depth, a surface area of 780 km^2, and a watershed area of 12,938 km^2. Lake Chaohu is geographically divided into two sections by Laoshan Island in the middle: the western lake (representing approximately 1/3 of the lake area) and the eastern lake (approximately. 2/3 of the lake area). The western lake is

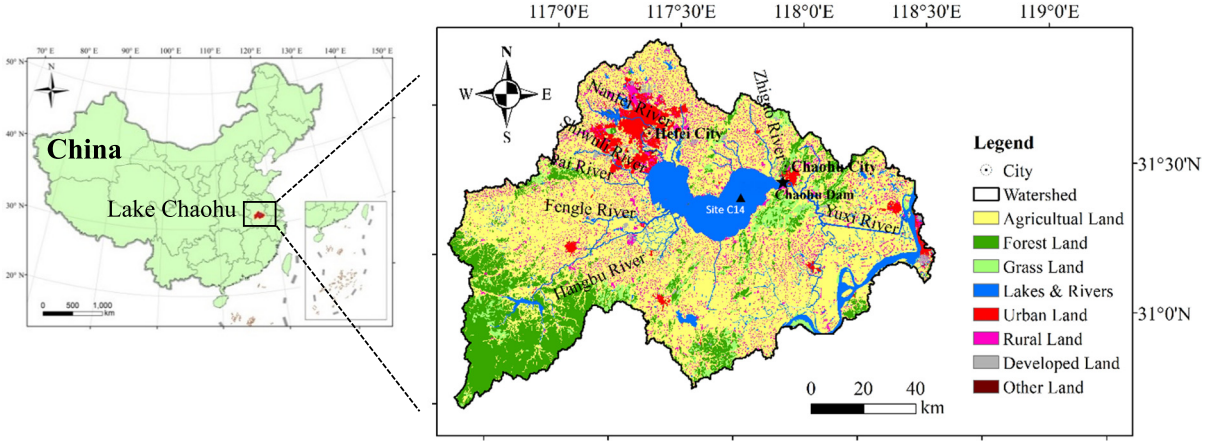

Fig. 1. Map of Lake Chaohu showing sediment core location.

surrounded by the city of Hefei (population of ~8×10^6 people) and the eastern lake by the city of Chaohu (population of ~1×10^6 people) (Zan et al., 2011). Seven primary tributaries discharge into the lake, providing ~80% of the runoff volume for the entire watershed. The lake's outlet, the Yuxi River, is the only channel connecting the eastern lake and the Yangtze River (Fig. 1). The lake became partially closed in 1963 and the outflow has been artificially controlled since then due to the construction of the Chaohu Dam on the Yuxi River in 1963. Lake Chaohu has played a significant role in supporting regional socioeconomic development by providing freshwater supply for consumption, crop irrigation and agricultural industry, fisheries, and other valuable ecosystem services. Lake Chaohu has been subject to extensive pollution and eutrophication in recent decades due to increasing human activities including fertilizer use and increasing development of urban and industrial areas. Discharge of untreated domestic and industrial wastewaters from surrounding cities is the principal source of pollutants into the lake (Zan et al., 2012). The sampling site, called C14, was targeted in the center of the eastern lake, sufficiently distal to stream inlets and the lake outlet to avoid sediment disturbance and resuspension (Fig. 1). Three sediment cores were collected at the same location in December 2017 using a gravity corer fitted with a PMMA tube (inner diameter of 8 cm, length of 50 cm). The three duplicate sediment cores were sampled and analyzed individually for the following methodologies: short-lived isotope dating, pigment analysis, and molecular analysis. After siphoning the overlying water from the sediment-water interface, the upper 30 cm of the cores were sectioned into 30 slices of 1 cm thickness. The samples were transported on dry ice to the laboratory. With the exception of the sub-samples used for molecular analysis, the samples were freeze-dried at −50 °C and ground with an agate mortar and pestle to homogenize, followed by passing through a 100 mesh (149 μm) sieve before analysis. For each molecular core subsample, 1 g from the center of each layer was used for DNA analysis to preclude potential contamination resulting from contact with the core sleeve wall. Samples were stored in 10 mL sterile centrifuge tubes at −80 °C in a black bag and were mixed well prior to analysis.

2.2. Dating and paleoenvironmental variable analyses

Previous studies have demonstrated that post deposition ^{137}Cs diffusion does not significantly change the position of ^{137}Cs accumulation maxima in sediments (Wan et al., 1987, 2005). In addition, one of the principle assumptions of the most commonly applied ^{210}Pb sediment dating method is that the flux of $^{210}Pb_{ex}$, which is derived from atmospheric fallout and sedimentation rates, is relatively constant. Thus, many researchers have reported accurate results in recent decades using ^{137}Cs and $^{210}Pb_{ex}$ dating to derive average sediment accumulation rates (Wan et al., 1987, 2005; Al-Masri et al., 2002; Su et al., 2014). Consequently, the sediment core collected at site C14 was dated using ^{137}Cs and ^{210}Pb fallout radionuclides, as described previously (see Zan et al., 2011 for details; site C14 in Zan's study corresponds to site C14 in this study). Peak ^{137}Cs activity in 1963 provides an important time calibration marker at site C14, leading to the determination of the average sediment accumulation rate as 0.247 g cm^{-2} y^{-1} for that sediment core. $^{210}Pb_{ex}$ dating was also used to calibrate the dating results. Based on the vertical distribution of $^{210}Pb_{ex}$, the average sedimentation rate at C14 was calculated using the constant flux, constant sedimentation model (i.e., the CFCS model) (Al-Masri et al., 2002; Wan et al., 2005) resulting in an estimated average sediment accumulation rate as 0.242 g cm^{-2} y^{-1}. The $^{210}Pb_{ex}$ and ^{137}Cs peak-based methods consistently assigned the age of the 22–23 cm layer in the sediment core as 1963. Moreover, a comparison between ^{137}Cs and $^{210}Pb_{ex}$ dating results yielded good agreement for sediment core ages (Fig. 2). Although age-depth models have inherent uncertainty, the chronology provides better understanding of the paleo-environmental history of the lake and a time-calibration to relate geochemical variation within the sediment core to historical events in the watershed (Zan et al., 2011, 2012).

Determination of other paleo-physicochemical and biological parameters from the same core site, including total nitrogen (TN), total phosphorus (TP), total organic carbon (TOC), carbon ($\delta^{13}C_{org}$) and nitrogen ($\delta^{15}N$) stable isotopes, particle size, and pigment compositions, are described in previous publication (Zan et al., 2012; Zhang et al., 2019a). The misalignment of sediment core sections caused by separate analyses is negligible at the century scale (Zhang et al., 2019b), and thus did not contribute to misalignment of these two datasets. TN was determined using a Vario El elemental analyzer (Elementar Corporation, Hanau, Germany). TP was extracted with 1 N HCl after igniting for 2 h at 500 °C and then measured using the ascorbic acid method (Zan et al., 2012). TOC was determined using a TOC analyzer (multi N/C 2100, Analytik Jena AG, Jena, Germany) after the samples were treated with 1 mol L^{-1} HCl to remove inorganic carbon, dried at 105–110 °C for 30 min (Komada et al., 2008). $\delta^{13}C_{org}$ and $\delta^{15}N$ were measured using an isotope-ratio mass spectrometer (Finnigan Delta Plusplus XP). For $\delta^{13}C_{org}$ analysis, the samples were pretreated with 1 M HCl to remove inorganic carbon. Results were expressed in standard per mill units, relative to international standards; AIR (for N) or Vienna-PeeDee Belemnite (V-PDB, for C). The sediment particle size distribution was measured using a Malvern Mastersizer S2000 laser particle size analyzer (Malvern Instruments Limited, Malvern, UK; measuring range of 0.02–2000 μm) (Mccabe, 1986). Pigments were extracted with acetone and characterized using an Agilent 1200 series high performance liquid chromatograph (HPLC) equipped with an auto-sampler (Model G1315C) and a diode-array detector (Agilent Technologies Inc., Palo Alto, CA, USA) (Zapata, 2000; Jiang et al., 2016). The water TP concentrations are those described in Chen et al. (2011); they were based on sedimentary fossil diatom assemblages in order to establish a diatom-inferred total phosphorus (DI-TP) transfer function. These paleo-physicochemical and -biological variables, including their vertical profiles, are described in greater detail in the Supporting Information (Fig. S2).

2.3. Molecular analyses

2.3.1. DNA extraction

Rigorous laboratory procedures were applied to prevent sample contamination and ensure the authenticity of results. The DNA extractions and polymerase chain reactions (PCRs) were carried out in a laminar flow hood that was sterilized with ultraviolet radiation for 30 min, followed by treatment with 6% sodium hypochlorite prior to molecular analyses. Total DNA was extracted from 0.5 g aliquots of wet sediment using the PowerSoil® DNA Isolation Kit according to the manufacturer's instructions (MoBio Laboratories, Carlsbad, California, USA). DNA extractions were conducted in batches of six samples, with a blank extraction as a control each time. All blanks were negative, thus validating our use of contamination control procedures.

2.3.2. PCR amplification and sequencing

The universal eukaryotic primers 960F (5′-GGCTTAATTTGACTCAAC RCG-3′) and NSR1438 (5′-GGGCATCACA GACCTGTTAT-3′) were used to amplify the V7 hypervariable region of sediment 18S rRNA genes, yielding ~260 bp-long fragments from ~50 ng of DNA extracts (Capo et al., 2017). PCRs were performed in 50 μL reaction mixtures containing 10 μL of buffer, 2 μL of Q5 High-Fidelity DNA Polymerase, 1.5 μL of each forward and reverse primer (10 μM stock), 1.0 μL of dNTPs, 10 μL of High GC Enhancer, and 24 μL of H_2O. After an initial denaturation at 94 °C for 10 min, amplifications were performed by 35 cycles of incubations for 1 min at 94 °C, 1 min at 55 °C, and 30 s at 72 °C, followed by a final extension at 72 °C for 10 min (Capo et al., 2016). The CYA359F (5′-GGGG AATYTTCCGCAATGGG-3′) and CYA781R (5′-GACTACWG GGGTATCTA ATCCCWTT) primers were used to quantify total cyanobacterial DNA and amplified a ~400 bp fragment of the V3 and V4 hypervariable regions of cyanobacterial 16S rRNA genes. The PCR conditions used for amplifying cyanobacterial 16S rRNA genes included an initial

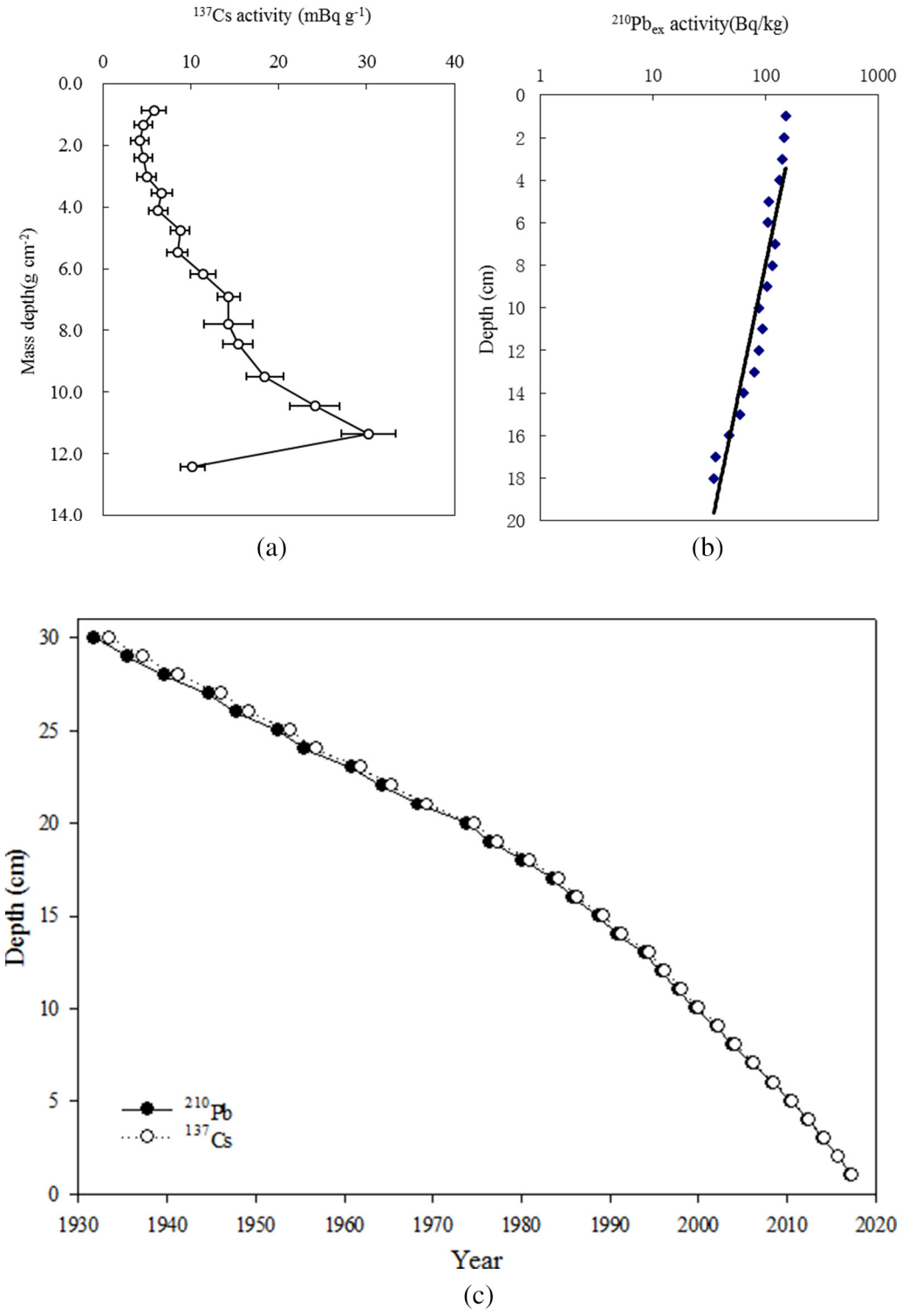

Fig. 2. ^{137}Cs (a) and $^{210}Pb_{ex}$ (b) vertical profiles of the sediment cores in Lake Chaohu. (c) The age-depth profile using short-lived isotopes.

denaturation for 5 min at 94 °C, followed by 35 cycles of 94 °C for 1 min, 60 °C for 1 min, and 72 °C for 1 min, followed by a final primer extension at 72 °C for 5 min (Nübel et al., 1997; Monchamp et al., 2016). The amplified products were purified and recovered using 1.8% agarose gel electrophoresis and gel extraction. The purified amplicons were sequenced on the Illumina HiSeq 2500 platform by BioMarker Technologies Co., Ltd. (Beijing, China).

2.3.3. Sequence data analyses

Paired-end raw sequence reads were first merged using FLASH (v1.2.7). The merged reads were compared to the PCR primer sequences using the FASTX-Toolkit, and reads with more than six mismatches to the primers were discarded. Reads with an average quality score of <20 over a 50 bp sliding window were truncated using Trimmomatic (v0.33), and reads trimmed to <300 bp were discarded. Putative

chimeric sequences were identified and removed using UCHIME (v4.2), as implemented in Mothur (v1.35.1). Quality filtered sequences were then clustered using the QIIME UCLUST module, wherein reads with nucleotide similarity of ≥97% were clustered into operational taxonomic units (OTUs). Taxonomy was assigned to eukaryotic algal OTUs by comparing representative sequences against the Silva database using the RDP classifier within QIIME. The cyanobacterial 16S rRNA gene sequences were also taxonomically identified via BLAST searches of representative sequences against the curated National Center for Biotechnology Information (NCBI) database.

2.4. Statistical data analyses

The OTU compositions for the eukaryotic algal and cyanobacterial libraries were statistically analyzed after normalizing for read depth across libraries. The OTU richness, Shannon, and Pielou indices were used to evaluate eukaryotic algal and cyanobacterial OTU alpha diversity. To identify whether significant changes occurred over time in each community's alpha diversity values, Bayesian change point analysis was used to estimate the posterior probabilities for the presence of inflection points, using the *bcp* package for R. Beta diversity was calculated based on the Bray-Curtis dissimilarity matrix and using the *vegan* package for R. The Beta diversity matrix was subjected to non-metric multi-dimensional scaling (NMDS) and Ward's cluster analysis to compare groups. The ANOSIM statistic was used to compare the means of community dissimilarities between groups to the means of community dissimilarities within groups. An ANOSIM R value close to 1.0 suggests high dissimilarity between groups, while an R value close to 0 suggests similar community dissimilarities within and between groups. R values <0 suggest that dissimilarities are greater within groups than between groups (Buttigieg and Ramette, 2014).

2.4.1. Correlation analyses

Spearman's correlation analysis was used to identify correlations between the relative abundances of individual eukaryotic algal and cyanobacterial groups and individual paleo-environmental variables (nutrients, particle sizes, and pigment compositions), and air temperature using the *corrplot* package for R. Only statistically significant ($p < 0.05$) correlations are shown. Previous studies have shown that surface air temperature and Lake surface water temperature day/night had the strongest correlation (Yang et al., 2020). Lake surface water temperatures have increased worldwide, which is similar to or in excess of air temperature trends (Woolway et al., 2020). Air temperature data for the years 1930–2012 were obtained from the Climatic Research Unit database (CRU, University of East Anglia; http://www.cru.uea.ac.uk/) with a horizontal resolution of 0.5° * 0.5°.

2.4.2. Random Forest model analyses

Random Forest (RF) classifications were used to determine the contributions of individual paleo-environmental variables to the alpha diversity (i.e., OTU richness and Shannon index) and structures (i.e., the axis 1 and 2 values of the NMDS plot) of the eukaryotic algal and cyanobacterial communities using the *ggRandomForest* package in R. RF analysis is an ensemble learning method for classifying or regressing data that operates by constructing a multitude of decision trees during training and outputting the class structure representing the mode of the classes or the mean prediction of the individual trees (Thomas et al., 2018). Thus, the RF algorithm is a powerful predictive tool that does not require pre-selection of variables to explain data structures. One thousand trees were used to construct the RF model. The order of importance of factors was estimated using nutrients, air temperature, and particle sizes as predictor variables and the diversity of eukaryotic algae and Cyanobacteria as the dependent variables within the eight output RF models.

2.4.3. Network analysis

Network analysis is a visualization method that can reveal correlations between biological population abundances and environmental parameters in complex communities. To understand the effects of environmental factors on species association networks, DI-TP concentrations and air temperature were also included in these network analyses. The adjacency matrices were calculated based on Spearman correlation values between each pair of OTUs using the *igraph* and *psych* packages for R. Network visualization and module detection of the co-occurrence relationships among eukaryotic algal and cyanobacterial OTUs were conducted using Gephi v 0.9.2 with the Frucherman Reingold placement algorithm.

2.4.4. Generalized additive model analysis

Generalized additive models (GAMs) were used to separate and quantify the impacts of human activities and climate warming on eukaryotic algal and cyanobacterial community succession (Capo et al., 2017). The general structure of the GAMs was:

$$g(\mu) = \beta_0 + \sum_{i=1}^{k} s_i(x_i) + \varepsilon$$

where μ is the response variable, β_0 is a constant intercept term, $s_i(x_i)$ is the smooth function of explanatory variable x_i, and ε is the residual with var. (ε) = δ^2. The Akaike information criterion (in terms of lowest AIC) and generalized cross validation (GCV) scores were used to select predictor variables and the evaluate their inclusion in models (Pearce et al., 2011). All GAMs were constructed using the 'mgcv' package for R.

3. Results and discussion

3.1. Historical succession of eukaryotic algal and cyanobacterial communities

High-throughput sequencing of environmental DNA extracted from Lake Chaohu sediments provided a taxonomically sensitive method to reconstruct historic eukaryotic algal and cyanobacterial community compositions. A total of 2,777,228 paired reads were obtained from 18S rDNA sequencing of 30 samples, with 456,968 clean reads clustered into 2752 OTUs after cleaning, clustering, and confirmation of eukaryotic algal taxonomic classification. In addition, a total of 2,389,351 paired reads were obtained by 16S rRNA gene sequencing of 30 samples, with 1,897,009 reads clustered into 2774 OTUs after quality filtering and classification as Cyanobacteria. OTUs classified as non-eukaryotic algal eukaryotes (e.g., metazoans, embryophytes, fungi, and protozoa) and non-Cyanobacteria bacteria were discarded from each library in order to only evaluate changes in eukaryotic algal and cyanobacterial community structures. These analyses yielded 117 eukaryotic algal OTUs and 56 cyanobacterial OTUs that were used in further analysis (Table 1).

Several limitations should be considered when conducting robust paleo-environmental DNA analyses (Capo et al., 2016; Monchamp et al., 2016). As described in the materials and methods section, rigorous laboratory procedures, strict analytical procedures, and stringent bioinformatics analyses were used to ensure the validity of molecular data. Moreover, DNA amplification using two different lengths of barcode primers has been previously used to evaluate the quality of preserved DNA in Lake Chaohu sediments (Capo et al., 2016; Monchamp et al., 2016). These previous studies have confirmed the capacity to sequence shorter DNA fragments of ~260 bp for eukaryotic algae and ~400 bp for Cyanobacteria, which could still be used to reconstruct historical trends in eukaryotic algal and cyanobacterial communities in Lake Chaohu.

Table 1
The table presents for the number of DNA sequences, OTUs within each eukaryotic algae and cyanobacteria group, and the percentage within each taxonomic group. Bold characters are used for the 9 and 8 most abundant taxonomic groups for eukaryotic algae and cyanobacteria, respectively.

	Taxonomic groups		DNA sequences	OTUs	Percentage (%)
Eukaryotic algae	Dinophyta	**Dinophyceae**	7233	17	5.583
	Cryptophyta	Cryptophyceae	744	4	0.574
	Haptophyta	Prymnesiophyceae	725	4	0.56
	Rhodophyta	Florideophyceae	413	2	0.319
	Bacillariophyta	**Mediophyceae**	13,393	8	10.337
		Bacillariophyceae	7664	5	5.915
		Coscinodiscophyceae	21,923	3	16.921
		Fragilariophyceae	5	2	0.004
	Chrysophyta	**Chrysophyceae**	11,697	29	9.028
	Ochrophyta	Dictyochophyceae	4	1	0.003
		Eustigmatophyceae	10,914	3	8.424
	Xanthophyta	Raphidophyceae	9	1	0.007
	Chlorophyta	**Trebouxiophyceae**	6383	10	4.927
		Chlorophyceae	43,724	22	33.747
		Zygnematophyceae	31	5	0.024
		Unclassified Chlorophyta	4702	1	3.629
Cyanobacteria	Chroococcidiopsidales	Chroococcidiopsis	7	2	0.006
	Nostocales	Aphanizomenon	70	1	0.058
		Cuspidothrix	72	1	0.06
		Cylindrospermopsis	1	1	0.001
		Dolichospermum	135	2	0.112
	Oscillatoriophycideae	Gloeocapsa	1	1	0.001
		Microcoleus	29	2	0.024
		Microcystis	47,213	1	39.119
		Planktothricoides	993	1	0.823
		Planktothrix	21	1	0.017
		Chroococcales	2574	2	2.133
		Unclassified oscillatoriales	35	4	0.029
	Synechococcales	**Cyanobium**	47,600	6	39.44
		Limnococcus	16	1	0.013
		Nodosilinea	2	1	0.002
		Oculatella	2	1	0.002
		Pseudanabaena	520	1	0.431
		Synechococcus	15,833	15	13.119
	Unclassified cyanobacteria		5567	12	4.613

3.1.1. Eukaryotic algal and cyanobacterial community compositions

A total of 117 OTUs comprising 129,564 reads were recovered and classified within 16 eukaryotic algal groups (Table 1). Among these, nine groups represented more than 98% of the total of eukaryotic algal DNA sequences (127,633 DNA sequences), including *Dinophyceae*, *Mediophyceae*, *Bacillariophyceae*, *Coscinodiscophyceae*, *Chrysophyceae*, *Eustigmatophyceae*, *Trebouxiophyceae*, *Chlorophyceae*, and unclassified *Chlorophyta* OTUs (Table 1). We primarily focused on the temporal dynamic of these nine dominant groups for further analysis, while the remaining seven low-abundance taxonomic groups were considered as 'other algae' (Table 1, Fig. 3a). *Chlorophyta* (comprising *Trebouxiophyceae*, *Chlorophyceae*, and unclassified *Chlorophyta*) and *Bacillariophyta* (*Mediophyceae*, *Bacillariophyceae*, and *Coscinodiscophyceae*) were the dominant groups, representing between 10.24%–67.74% and 6.31%–68.25% of the total eukaryotic algal reads per sample, respectively (Fig. 3a). A previous analysis of phytoplankton community structural changes at the decade scale using Lake Chaohu sedimentary pigments also observed diatoms and green algae as the historically dominant phytoplankton groups (Zhang et al., 2019a). Sedimentary pigment characterization has often been used to reconstruct historical algal community compositions at the phylum level and evaluate historical changes in phytoplankton biomass (Deshpande et al., 2014; Tse et al., 2015; Jiang et al., 2016). As described here, sedimentary genetic analysis can also be used as a complementary approach that could provide more detailed taxonomic information of historic populations (Savichtcheva et al., 2015; Domaizon et al., 2017; Li et al., 2019). Moreover, sedimentary DNA sequencing and pigment analyses can serve as historical proxies of past lacustrine primary production (Pal et al., 2015; Tse et al., 2018).

Diverse cyanobacterial communities were observed after 16S rRNA amplification with cyanobacterial-specific primers of 30 sediment DNA samples spanning ~90 years. After removing non-cyanobacterial sequences, 56 cyanobacterial OTUs comprising 120,691 reads were assigned to 18 phylogenetic groups (Table 1). The 40 most abundant OTUs represented more than ~99% of the total cyanobacterial sequence reads (120,435 DNA sequences) and were associated with eight taxonomic groups including the *Dolichospermum*, *Microcystis*, *Planktothricoides*, *Chroococcales*, *Cyanobium*, *Pseudanabaena*, *Synechococcus*, and unclassified *Cyanobacteria* (Table 1). The remaining ten low-abundance taxonomic groups were considered as 'other Cyanobacteria' (Table 1, Fig. 3b). *Microcystis* and *Cyanobium* were the predominant cyanobacterial taxa, with average relative abundances of 33.85% and 40.20%, respectively. These results are consistent with a previous investigation of Lake Chaohu during 2011–2012, wherein *Cyanophyta* represented 51.2% of the total 97 phytoplankton species observed in Lake Chaohu, with *Microcystis viridis* and *Microcystis flos-aquae* as the dominant species (Jiang et al., 2014). The average relative abundance of *Synechococcus* was 13.12% in the sedimentary DNA libraries (Fig. 3b), which represents a more accurate estimate than underestimations previously observed with microscopy (Deng et al., 2007; Jiang et al., 2014). This discrepancy arises because several species in the *Synechococcus* genus are unicellular picocyanobacteria with diameters <2 μm and are difficult to identify by microscopy-based morphological observations (Dvořak et al., 2014; Monchamp et al., 2016).

It should be noted that the reconstruction of lake phytoplankton communities based on relatively long DNA markers that exist in sedimentary archives may be biased due to DNA degradation that occurs with increasing sediment age (Barnes et al., 2014; Pal et al., 2015; Monchamp et al., 2018). To evaluate this potential bias, the sequence libraries in the present study were carefully inspected and significant biases in taxonomic representation were not detected, as evinced by the lack of OTU disappearance in specific layers with increasing

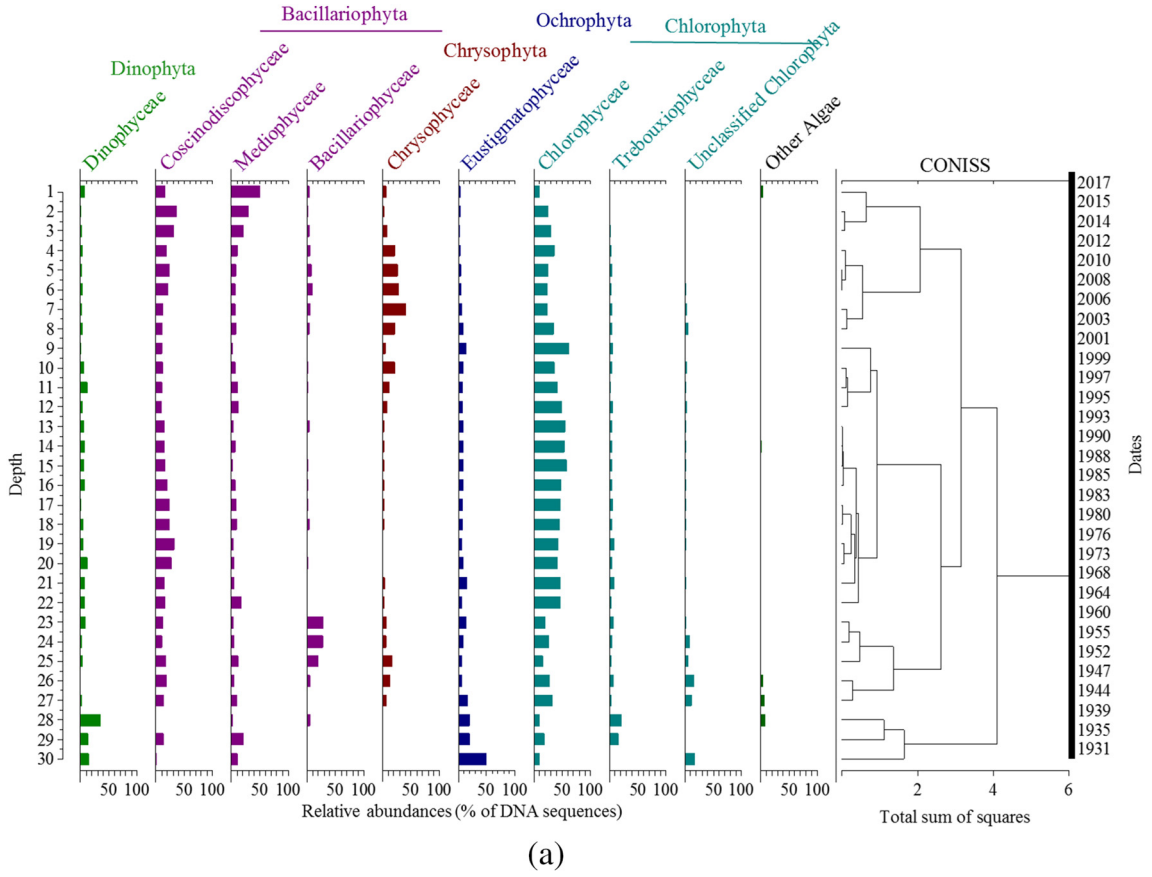

Fig. 3. Temporal relative abundances of the eukaryotic algae (a), and cyanobacteria (b) taxonomic group over time at Lake Chaohu. In the right part of the graph showing the result of Constrained Incremental Sums of Squares Cluster Analysis (CONISS) based on the relative abundance of eukaryotic algae and cyanobacteria group in terms of DNA sequences of different layers.

sediment age (Monchamp et al., 2018). Moreover, the reconstructed eukaryotic algal and cyanobacterial community compositions identified here are consistent with those inferred by historical microscopy of water samples (Deng et al., 2007; Jiang et al., 2014). For example, *Cyanophyta*, *Chlorophyta*, and *Bacillariophyta* represented 35.4%, 34.2%, and 17.7% of the 97 identified phytoplankton species in Lake Chaohu, respectively, based on microscopy of water samples (Jiang et al., 2014).

3.1.2. Temporal patterns in eukaryotic algal and cyanobacterial community diversity

The OTU richness of eukaryotic algal communities varied from 15 to 81 OTUs in the Lake Chaohu sediment core samples, with a total observed richness of 1401 OTUs. The Shannon diversity and Pielou evenness indices of eukaryotic algal communities ranged from 6.56 to 25.29 and 0.15 to 0.65 over the past nearly 9 decades, respectively (Fig. 4A). The major inflection points for compositional changes in eukaryotic algal communities were inferred as between the 1960s and 2000s based on CONISS analysis (Fig. 3a). This change coincides with significant variation in alpha diversity metrics (i.e., OTU richness, Shannon index, and Pielou index values), based on Bayesian change point (*bcp*) analysis (Fig. 4A).

The OTU richness of cyanobacterial communities varied from 17 to 41 OTUs in the sediment core samples, with a total observed richness of 771 OTUs. The Shannon diversity and Pielou evenness indices ranged from 2.65 to 11.56, and 0.11 to 0.58 over the past nearly 9 decades, respectively (Fig. 4B). The main inflection point for changes in cyanobacterial community structures was inferred between 1968 and 1973 based on CONISS analysis (Fig. 3b). Thus, this estimated critical period of cyanobacterial community change followed construction of the Chaohu Dam. OTU richness generally increased after this point, while the diversity and evenness estimates based on the Shannon and Pielou indices, respectively, remarkably decreased around the mid-1970s (Fig. 4B). These results suggest that changes in alpha diversity lagged behind those of community structure, indicating asynchronism between changes in community diversity and structure over longer time scales (Li et al., 2019). Consistently, recent studies have observed that diversity indices, as integrations of all species information for a community, may ignore changes in community structure, and is therefore sometimes less sensitive to environmental changes (Spaak et al., 2017; Li et al., 2019).

The continual changes in eukaryotic algal and cyanobacterial communities over time were evident following NMDS analyses based on Bray-Curtis community distances (Fig. 5). These structural changes also coincided with positive increases in DI-TP concentrations and air temperatures. Consistently, recent studies have suggested that phosphorous concentrations and air temperatures are two primary forcing factors that contribute to changes in eukaryotic algal and cyanobacterial community structures in European peri-Alpine lakes (Savichtcheva et al., 2015; Capo et al., 2017; Monchamp et al., 2018).

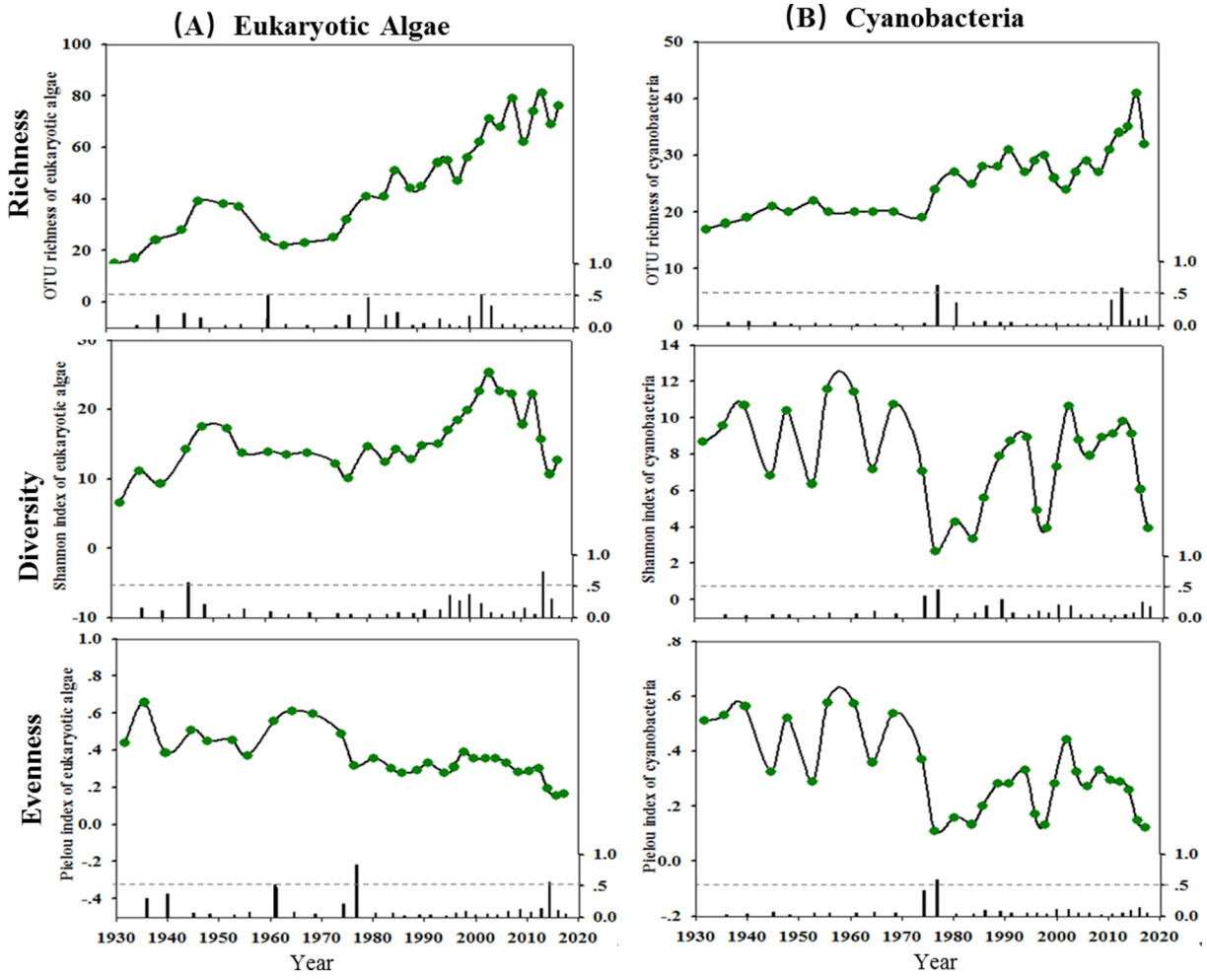

Fig. 4. Time series of richness (operational taxonomic unit richness), diversity (Shannon index), and evenness (Pielou index) indices for eukaryotic algae (A) and cyanobacterial (B) communities at Lake Chaohu. In the upper part of graph, the line with scatter reflects the temporal trend of the index. The bar graph is the posterior probability value by *bcp* analysis. Horizontal gray dotted lines indicate that the posterior probability value equal or superior to 0.5 that is considered as a significant change point.

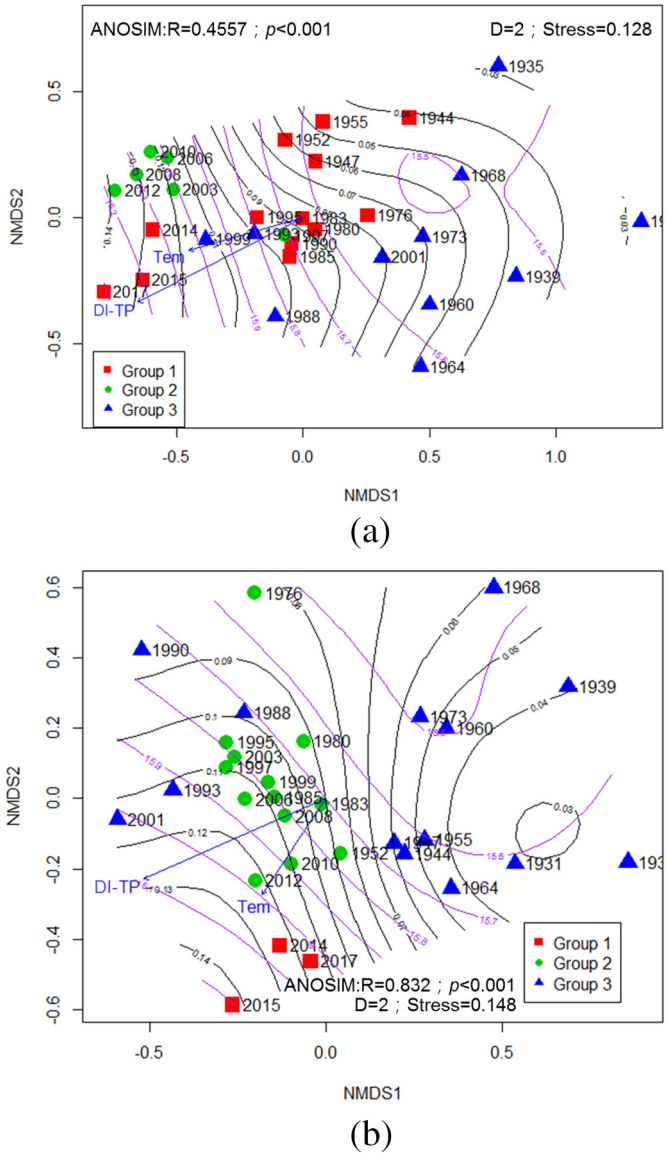

Fig. 5. Non-metric multi-dimensional scaling (NMDS) analysis and Ward cluster analysis of eukaryotic algae (a), and cyanobacteria (b) communities based on Bray-Curtis dissimilarity. Gradient of diatom-inferred total phosphorus (DI-TP) concentration (black line) and air temperature (purple line) were plotted with community structure data. The ANOSIM statistic compares the mean of ranked dissimilarities between groups to the mean of ranked dissimilarities within groups. (For interpretation of the references to colour in this figure legend, the reader is referred to the web version of this article.)

3.2. Historical dynamics of community changes and the relative importance of forcing factors

The temporal dynamics of eukaryotic algal and cyanobacterial communities in Lake Chaohu may be driven by diverse environmental forcing factors, including nutrient enrichment, climate warming, and changes in lake hydrodynamics (Zhang et al., 2019a). The eutrophication of Lake Chaohu has been driven by enhanced anthropogenic nutrient inputs due to increased population sizes and fertilizer use in the drainage area, as well as altered hydrologic conditions after construction of the Chaohu Dam (Chen et al., 2011; Zan et al., 2012). Land use types in the polders have dramatically changed between 1988 and 2015 (Fig. S3; Table S1). Specifically, agricultural land area in the basin decreased by 769.24 km^2 (5.39% of the total area) between 1988 and 2015, while urban and rural land areas increased by 367.83 and 263.79 km^2 (2.58% and 1.85% of the total area), respectively.

Sedimentary nutrient proxies, including TN, TP, and TOC, increased after the 1960s, while co-occurring $\delta^{13}C$ and $\delta^{15}N$ values indicated that organic matter was predominantly sourced by algae and that primary productivity increased over this period (Fig. S1). Diatom successional patterns and historical DI-TP trends have previously indicated that Lake Chaohu experienced obvious eutrophication trends following the 1970s (Fig. S2; Chen et al., 2011). Moreover, changes in grain size components (i.e., fine grains increased and coarser grains decreased after 1963) provide evidence for stable depositional conditions due to sharp decreases in water exchange volumes following the construction of Chaohu Dam (Fig. S1; Zan et al., 2012). The relationship between hydrodynamic conditions and sediment particle size was explored by Zan et al. (2012), demonstrating that particle size distribution became more finely skewed after dam construction. Therefore, lowered discharge and/or trapping of coarse particles culminated in fine particle sedimentation in Lake Chaohu. Further, nutrient loading has accelerated in the lake after the 1970s as a consequence of large amounts of industrial, agricultural, and domestic sewage that has been discharged into Chaohu Lake (Zan et al., 2012).

The relative abundances of the eukaryotic algal group *Chlorophyceae* as well as the cyanobacterial taxa *Dolichospermum*, *Microcystis*, *Planktothricoides*, *Cyanobium*, *Pseudanabaena*, and *Synechococcus* were significantly and positively correlated with DI-TP concentrations and $\delta^{15}N$ in addition to sedimentary TN, TP, and TOC concentrations based on Spearman's correlational analysis ($p < 0.05$; Fig. 6). Increasing eutrophication driven by anthropogenic activities has been considered the major factor that drives lacustrine biological community succession (Häder and Gao, 2014; Paerl et al., 2016). Thus, nutrient enrichment resulted in excessive algal growth and especially of Cyanobacteria and *Chlorophyceae*, which is consistent with sedimentary pigment analyses of Lake Chaohu and their inferred historical abundances via pigments (Zhang et al., 2019a).

The succession of algal communities in Lake Chaohu was likely driven in part by major changes in lake hydrodynamics, including decreased discharge to/from the lake after completion of the Chaohu Dam in 1963 (Chen et al., 2011; Zan et al., 2012). Sedimentary grain size components provide important information on hydrologic changes due to the relationship between the transport of different grain sizes with hydrodynamic intensity (Xue et al., 2010; Zeng et al., 2018). The grain sizes in Lake Chaohu sediments markedly decreased after dam construction, reflecting the inferred contemporaneous hydrologic changes (Zan et al., 2012). The increased prevalence of fine particles (<8 μm) after this time clearly indicates that hydraulic residence times significantly increased following dam completion, as would be expected. In addition, significant and positive correlations were observed between the proportions of fine grain sizes (<4 μm and 4–8 μm) and *Dolichospermum*, *Microcystis*, *Planktothricoides*, *Cyanobium*, *Pseudanabaena*, and *Synechococcus* abundances. In addition, significant and negative correlations were observed between the proportions of grain sizes larger than 8 μm (8–16 μm and 16–64 μm) and these same taxa ($p < 0.05$; Fig. 6). These results provide evidence that longer hydraulic residence times may facilitate the proliferation of these cyanobacterial groups, thereby driving shifts in the structures and compositions of their communities (Zeng et al., 2018). These results are consistent with previous observations that damming can have a direct metabolic effect on phytoplankton, but also indirect effects that are mediated by physical (e.g., long hydraulic residence times leading to less mixing) and chemical (e.g., nutrient enrichment due to retention) dynamics (Maavara et al., 2015 & 2017; Zeng et al., 2018).

The connection between lacustrine ecosystem structures and anthropogenic-driven changes are widely acknowledged. However, the influence of rising temperatures is a growing concern in the context of lake ecological changes (Michalak et al., 2016; O'Beirne et al., 2017). The annual average temperature within the Lake Chaohu watershed

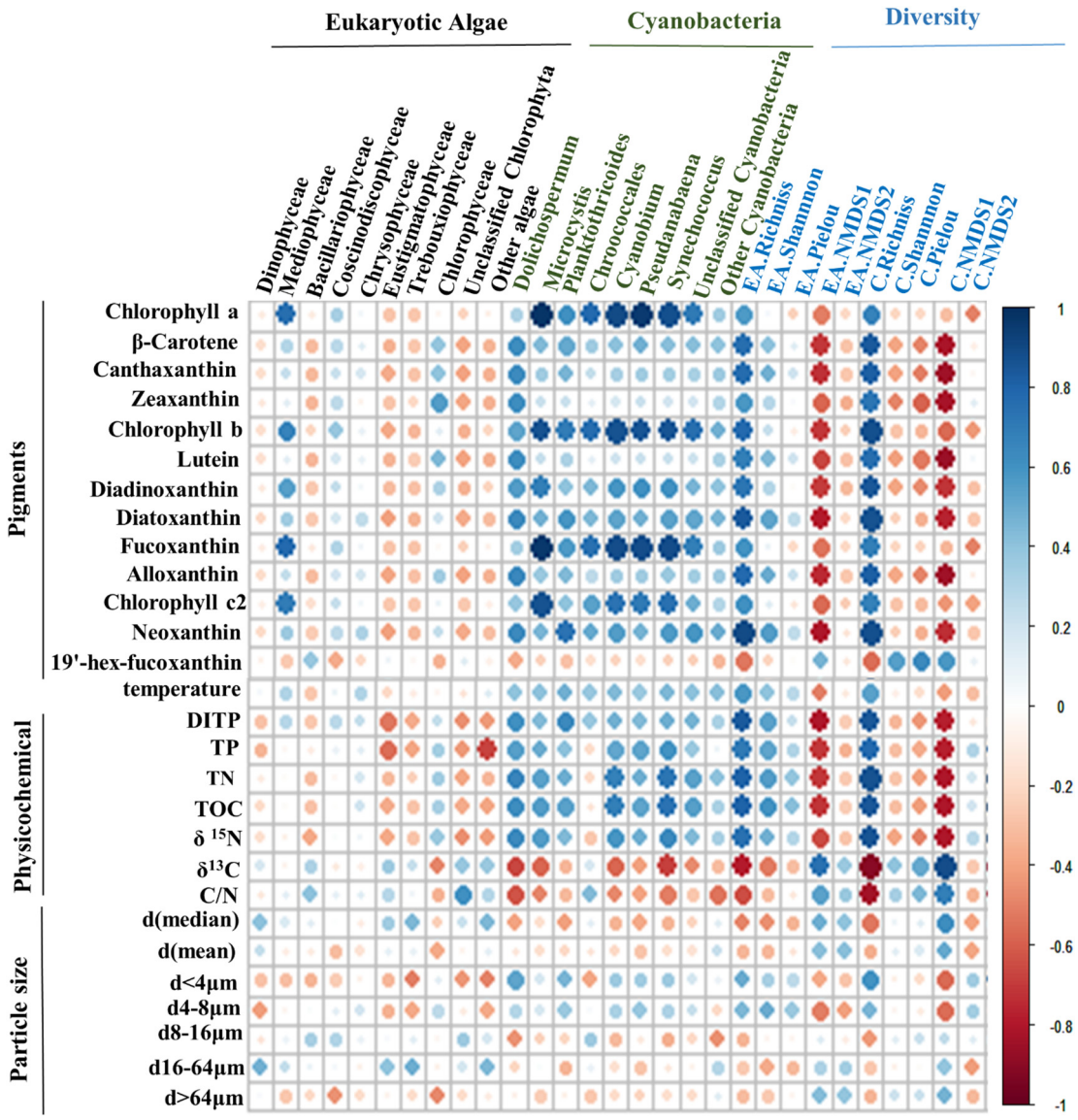

Fig. 6. Spearman's ranked correlation coefficients between the relative abundances of individual groups, the alpha (OTU richness, Shannon and Pielou index), and beta diversity (the value of axis 1 and axis 2 of NMDS plot) of eukaryotic algae and cyanobacteria, and individual proxies (physicochemical, particle size and pigments). Larger and darker circles indicate robust correlations. Only correlations that are statistically significant ($p < 0.05$) are shown.

increased by 0.69 °C between 1930 and 2012 ($p < 0.01$) and has significantly increased following the 1990s (Fig. S4). Mean lake temperature was significantly and positively correlated with the abundances of all cyanobacterial groups and some eukaryotic algal groups (Fig. 6). Climate warming prediction studies of phytoplankton have generally indicated that the temperature optima for cyanobacterial photosynthesis and growth are higher than those of eukaryotic algae, thereby creating a competitive advantage for Cyanobacteria under warming conditions (Caron and Hutchins, 2013; Helbling et al., 2015; O'Beirne et al., 2017). Importantly, the toxins produced by Cyanobacteria like *Microcystis* are serious threats to water resources and lacustrine ecosystems (Michalak et al., 2016; Paerl et al. 2016 & 2019) and would thus be expected to become more prevalent under warmer climate regimes.

The structures and compositions of lacustrine biological communities are influenced by complex and varied environmental factors (Smol et al., 2005; Savichtcheva et al., 2015). Active debate has focused on how drivers, including nutrient levels, dam construction, and climate change, can alter lacustrine biological communities, and studies have evaluated the factors that play the most important roles in changing communities (Smol et al., 2005; Stager et al., 2018). For example, it is unclear whether phosphorous-only or combined nitrogen-and-phosphorous management strategies are most effective for mitigating cyanobacterial blooms in lake ecosystems (Paerl et al. 2016 & 2019). To investigate how different species have adapted to nutrient loading and changes in other physiochemical variables in Lake Chaohu over the last nearly 90 years, a RF machine learning algorithm was used to quantify the relative importance of environmental variables in predicting the diversity and structures of eukaryotic algal and cyanobacterial communities (Fig. 7). DI-TP concentrations and other sedimentary geochemical proxies (i.e., TN, TOC, and the C/N ratio) were generally the most important parameters for predicting Lake Chaohu eukaryotic algal community characteristics (Fig. 7A). In contrast, hydraulic residence times, as indicated by average and median grain sizes, was more important for predicting cyanobacterial community characteristics in the lake. Further, cyanobacterial communities were more sensitive to changes in hydraulic residence times than to DI-TP concentrations, TN, and TP, as demonstrated by the smaller importance of the latter variables (Fig. 7B). Lastly, air temperature

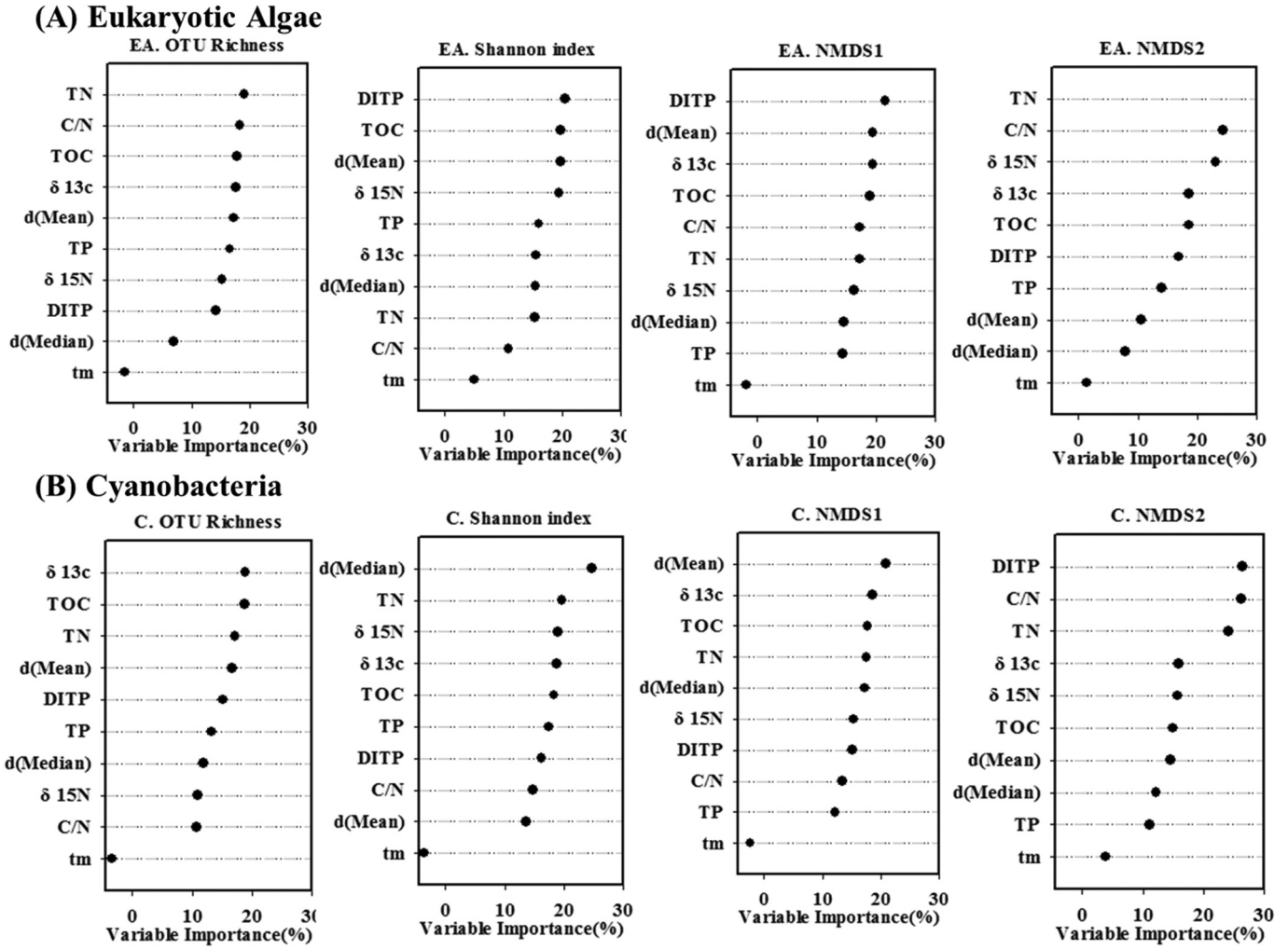

Fig. 7. Random Forest (RF) model of individual environmental variables on the diversity (OTU richness, Shannon diversity index, the value of axis 1 and axis 2 of NMDS plot) of eukaryotic algae (A) and cyanobacteria (B) in Lake Chaohu. The environmental variables include sedimentary TP, TN, and TOC concentration, $\delta^{15}N$ and $\delta^{13}C$ values, C/N ratios, median and mean particle size (d(median) & d(mean)), diatom-inferred total phosphorus concentration (DI-TP) and air temperature (tm).

explained the least amount of variance in eukaryotic algal and cyanobacterial communities relative to the other variables (Fig. 7).

3.3. Contributions of environmental drivers to changes in phytoplankton communities

Quantifying the impacts of environmental drivers can help better inform the responses of lacustrine phytoplankton communities to human activities and climate warming, as well as in developing reasonable and effective lake protection strategies (Capo et al., 2017; Stager et al., 2018). Nevertheless, it is a challenge to define and separate the complex associations and interactions between climate, anthropogenic activities, and individual hydrologic processes (Häder and Gao, 2014; Mwangi et al., 2016). To begin to assess these dynamics, the potential effects of aquatic phosphorus concentrations (DI-TP), average grain sizes (d_{Mean}), and air temperature (tm) on the diversity (OTU richness and Shannon index values) and structures (axis 1 and axis 2 values of NMDS plots) of eukaryotic algal and cyanobacterial communities were determined using GAM analysis (Fig. 8; Table 2). DI-TP concentrations contributed to 67.14% and 53.95% of the variation in OTU richness and Shannon index values of eukaryotic algal communities, respectively, in addition to 72.46% and 54.15% of the variation in cyanobacterial communities, respectively (Table 2). The negative effects of DI-TP concentrations on the OTU richnesses of eukaryotic algal and cyanobacterial communities switched to positive effects after the 1970s (Fig. 8). Consistently, the contributions of DI-TP concentrations to eukaryotic algal and cyanobacterial community structures (i.e., NMDS axes scores) remarkably changed around the 1970s (Fig. 8). Thus, increased total phosphorus concentrations were associated with marked changes in eukaryotic algal and cyanobacterial communities over the past few decades.

Average grain size contributed mostly over 20% to variation in the OTU richness and Shannon index values of eukaryotic algal and cyanobacterial communities (Table 2). However, the effects of average grain size on these values increased after the 1960s (Fig. 8). These changes were concomitant with changes in lake hydrology driven by dam construction, thereby resulting in increased OTU richnesses for both eukaryotic algal and cyanobacterial communities (Zhang et al., 2019a).

The contributions of air temperature to the OTU richness and Shannon index values of eukaryotic algal communities were 8.72% and 18.35%, respectively, and 7.54% and 19.91% to cyanobacterial communities, respectively (Table 2). Thus, air temperature was a less influential predictor variable than hydrologic conditions and DI-TP concentrations for both eukaryotic algal and cyanobacterial communities in Lake Chaohu. The effects of air temperature on these values slightly increased following the 2000s (Fig. 8), indicating a relatively stronger impact on phytoplankton after the early 2000s. Climate warming can influence aquatic biological communities both directly and indirectly (Savichtcheva et al., 2015; Capo et al., 2017). For example, intensified

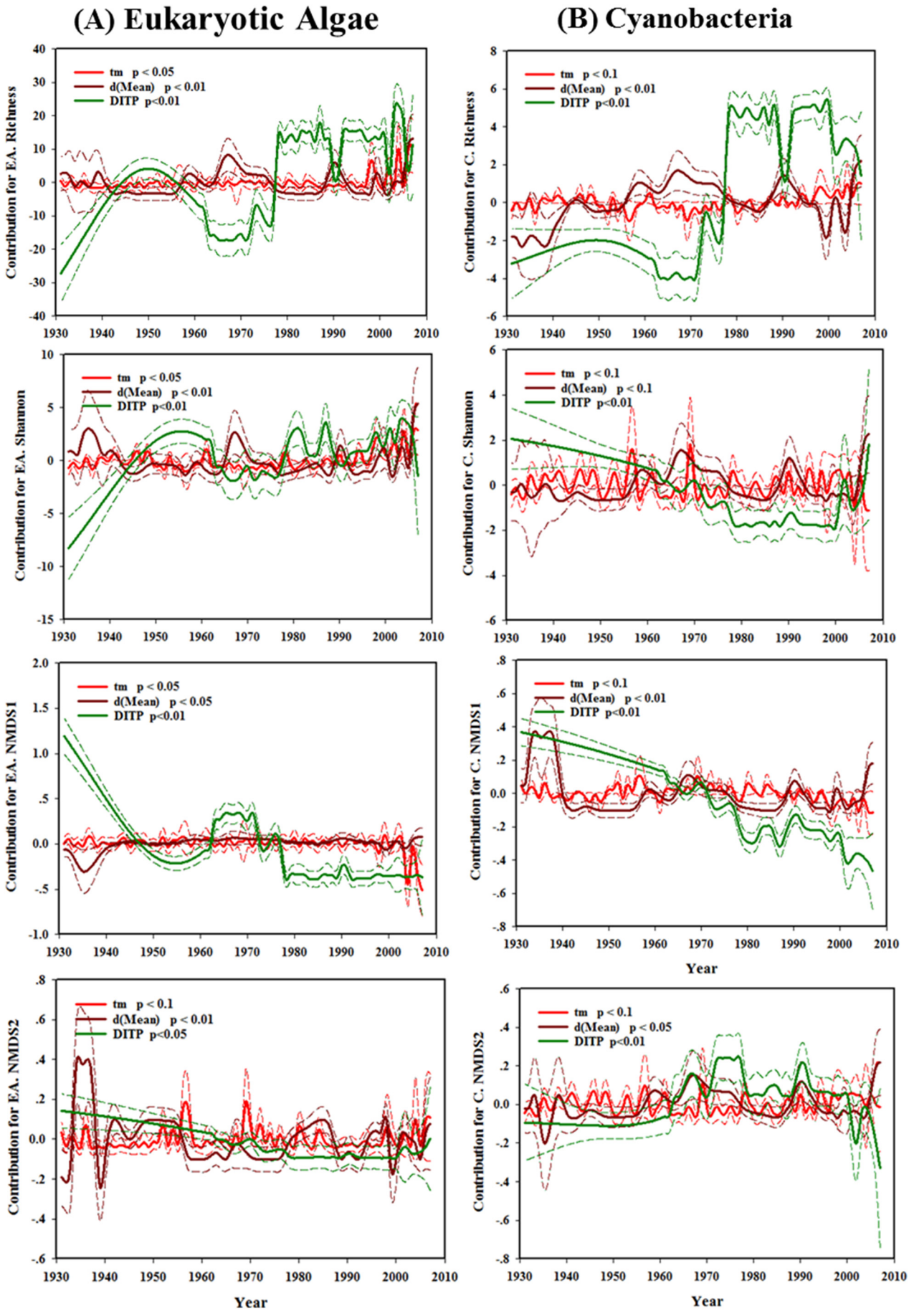
(A) Eukaryotic Algae
(B) Cyanobacteria
Contribution for EA. Richness
tm p < 0.05
d(Mean) p < 0.01
DITP p<0.01
Contribution for C. Richness
tm p < 0.1
d(Mean) p < 0.01
DITP p<0.01
Contribution for EA. Shannon
tm p < 0.05
d(Mean) p < 0.01
DITP p<0.01
Contribution for C. Shannon
tm p < 0.1
d(Mean) p < 0.1
DITP p<0.01
Contribution for EA. NMDS1
tm p < 0.05
d(Mean) p < 0.05
DITP p<0.01
Contribution for C. NMDS1
tm p < 0.1
d(Mean) p < 0.01
DITP p<0.01
Contribution for EA. NMDS2
tm p < 0.1
d(Mean) p < 0.01
DITP p<0.05
Contribution for C. NMDS2
tm p < 0.1
d(Mean) p < 0.05
DITP p<0.01
Year
Year

Table 2
GAMs analysis results for Eukaryotic Algae (EA) and Cyanobacteria (C) community in Lake Chaohu.

Models	P	R^2	Deviance explained	Contribution of predictor variables (%)		
				DITP	tm	d(Mean)
EA.Richniss~s(DITP,k = 10) + s(tm,k = 4) + s(d.Mean.,k = 5)	$P < 0.001$	0.856	88.50%	67.14	8.72	24.14
EA.Shannon~s(DITP,k = 8) + s(tm,k = 3) + s(d.Mean.,k = 6)	P < 0.001	0.664	72.10%	53.95	18.35	27.70
EA.NMDS1 ~ s(DITP,k = 8) + s(tm,k = 7) + s(d.Mean.,k = 5)	P < 0.001	0.873	89.60%	74.72	13.57	11.71
EA.NMDS2 ~ s(DITP,k = 3) + s(tm,k = 3) + s(d.Mean.,k = 6)	P < 0.05	0.455	51.30%	38.29	20.21	41.50
C.Richniss~s(DITP,k = 7) + s(tm,k = 3) + s(d.Mean., k = 3)	P < 0.001	0.86	87.60%	72.46	7.54	20.00
C.Shannon~s(DITP,k = 4) + s(tm,k = 4) + s(d.Mean.,k = 5)	P < 0.001	0.429	49.10%	54.15	19.91	25.94
C.NMDS1 ~ s(DITP,k = 3) + s(tm,k = 3) + s(d.Mean.,k = 4)	P < 0.001	0.77	78.70%	63.12	12.07	24.81
C.NMDS2 ~ s(DITP,k = 8) + s(tm,k = 4) + s(d.Mean.,k = 4)	P < 0.001	0.49	56.70%	50.37	20.10	29.54

Table 3
Properties of the two individual networks built for eukaryotic algae and cyanobacteria in Lake Chaohu.

Metrics	Eukaryotic algae	Cyanobacteria
Number of nodes	119	58
Nmber of edges	707	412
Average degree	11.882	14.207
Diameter	6	4
Density	0.101	0.249
Weighted modularity	0.456	0.2
Number of modules	11	10
Clustering coefficient	0.573	0.741
Average path length	2.686	1.83

The topological indices were calculated considering only the edges values superior to 0.5.

thermal stratification of lakes caused by climate change can exacerbate lake anoxia and enhance the growth of planktonic, bloom-forming cyanobacteria (Banjamin et al., 2015; Monchamp et al., 2018). Consequently, climate warming may play a prominent role in altering the compositions and structures of lacustrine algal communities in the future, leading to stressed ecosystems and potential health impacts from harmful algal blooms (O'Neil et al., 2012).

To explore the effects of environmental factors on species-species association networks, network analyses were conducted using the eukaryotic algal and cyanobacterial community compositional data. The resulting network consisted of 119 nodes linked by 707 edges for eukaryotic algal communities, and 58 nodes linked by 412 edges for cyanobacterial communities (Table 3). DI-TP concentrations were directly connected to OTU nodes by 30 and 24 edges in the eukaryotic algal and cyanobacterial networks, respectively. In addition, air temperature was directly connected to OTU nodes by 11 and 16 edges in these networks, respectively (Fig. 9). Specific OTUs assigned to the eukaryotic algal groups *Chlorophyceae*, *Trebouxiophyceae*, *Chrysophyceae*, *Dinophyceae*, *Bacillariophyceae*, and *Mediophyceae* in addition to cyanobacterial groups comprising *Microcystis*, *Planktothricoides*, *Cyanobium*, *Synechococcus*, and *Pseudanabaena* were associated with DI-TP concentrations. In addition, specific OTUs assigned to the eukaryotic algal groups *Dinophyceae*, *Chrysophyceae*, *Trebouxiophyceae*, and *Mediophyceae* along with cyanobacterial OTUs classified as *Cyanobium*, *Synechococcus*, *Pseudanabaena*, *Dolichospermum* were associated with air temperature (Fig. 9). Network analysis was also used to identify co-occurrence patterns among eukaryotic algal and cyanobacterial taxa (Tse et al., 2018). The majority of OTUs within the same identified modules may exhibit close positive relationships via, for example, co-occurrence (Zhao et al., 2016). The non-random co-occurrence patterns between taxonomically related eukaryotic algae or cyanobacteria can result from taxa sharing similar ecological niches or otherwise via taxa engaging in cooperative relationships (Zhao et al., 2016; Tse et al., 2018; Mandakovic et al., 2018).

4. Conclusions

Here, we apply high-throughput sequencing of sedimentary DNA to reconstruct the historical diversity of lacustrine eukaryotic algal and cyanobacterial communities. Moreover, we compared the reconstructed historical communities to multiple proxies for environmental processes to evaluate historical controls on ecosystem health. We further compare the reconstructed algal and cyanobacterial communities to multiple environmental proxies to evaluate the historical influences on ecosystem health. The results support our hypothesis that dam construction and nutrient enrichment affected the richness and diversity of eukaryotic algal and cyanobacterial communities starting in the 1960s.

Increased hydraulic resistance times and phosphorous enrichment were the major drivers of changes in eukaryotic algal and cyanobacterial communities over time, as mediated by the construction of Chaohu Dam in 1963 and the rapid eutrophication of the lake after the 1980s. Although rising air temperature played a lesser role than hydrologic conditions and nutrient enrichment on the algal/cyanobacterial communities of Lake Chaohu since the 1960's, it is imperative to consider that projected regional warming and climate change can couple with other human impacts in the future to exacerbate ecological stress.

CRediT authorship contribution statement

Hanxiao Zhang: Software, Data curation, Writing - original draft, Visualization, Investigation. **Shouliang Huo:** Conceptualization, Methodology, Supervision, Validation, Writing - review & editing. **Kevin M. Yeager:** Writing - review & editing. **Fengchang Wu:** Writing - review & editing.

Declaration of competing interest

The authors declare that they have no known competing financial interests or personal relationships that could have appeared to influence the work reported in this paper.

Acknowledgements

The National Key Research and Development Program of China (No. 2017YFA060500 3) and the National Natural Science Foundation of China (No. 51922010, 91751114) supported this study.

Fig. 8. GAMs analysis results for eukaryotic algae, and cyanobacteria communities in Lake Chaohu. The figure presents the contribution of diatom-inferred total phosphorus concentration (DI-TP, green line), the average particle size (d(Mean), brown line) and air temperature (tm, red line) to the eukaryotic algae (A) and cyanobacteria (B) community temporal changes considering OUT richness, Shannon diversity index, Pielou evenness index, and the value of axis 1 and axis 2 of NMDS plot. (For interpretation of the references to colour in this figure legend, the reader is referred to the web version of this article.)

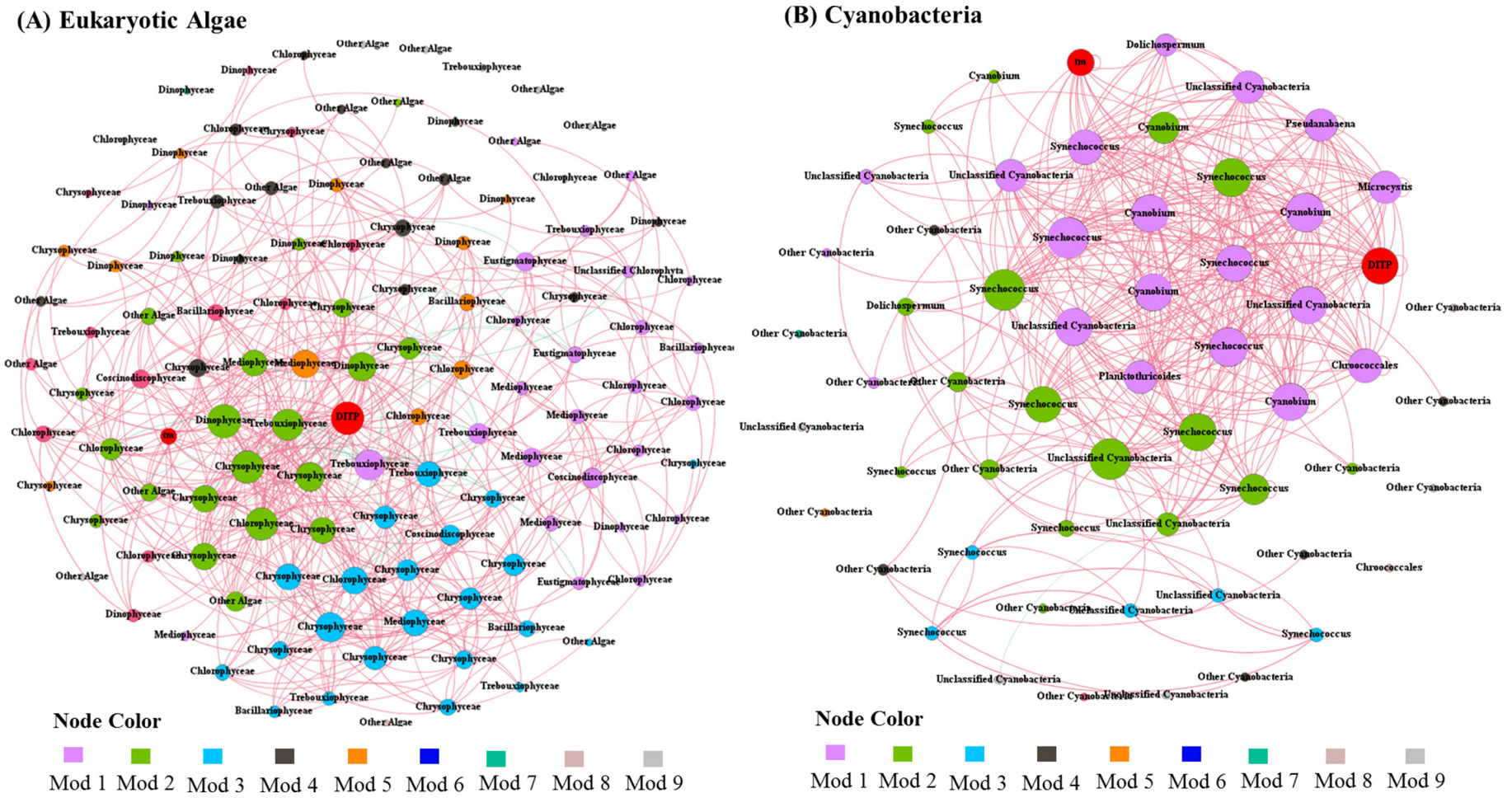

Fig. 9. Co-occurrence networks for Lake Chaohu eukaryotes and cyanobacteria communities. Each node represents one OTU, and the edges correspond to robust and significant correlations ($|\rho| > 0.5$ and $p < 0.05$) between nodes. The pink line signifies a positive correlation, and the green line signifies negative correlation. The nodes were colored by modularity class. Environmental variables: DI-TP: diatom-inferred total phosphorus concentration; tm: air temperature. (For interpretation of the references to colour in this figure legend, the reader is referred to the web version of this article.)

Appendix A. Supplementary data

Supplementary data to this article can be found online at https://doi.org/10.1016/j.scitotenv.2020.141985.

References

Al-Masri, M.S., Aba, A., Khalil, H., Al-Hares, Z., 2002. Sedimentation rates and pollution history of a dried lake: Al-Oteibeh Lake. Sci. Total Environ. 293, 177–189.

Banjamin, M.K., Orlane, A., Sudeep, C., Margaret, D., Esko, K., David, M.L., 2015. Morphometry and average temperature affect lake stratification responses to climate change. Geophys. Res. Lett. 42, 4981–4988.

Barnes, M.A., Turner, C.R., Jerde, C.L., Renshaw, M.A., Chadderton, W.L., Lodge, D.M., 2014. Environmental conditions influence eDNA persistence in aquatic systems. Environmental Science & Technology 48 (3), 1819–1827.

Blois, J.L., Zarnetske, P.L., Fitzpatrick, M.C., Finnegan, S., 2013. Climate change and the past, present, and future of biotic interactions. Science 341 (6145), 499–504.

Buttigieg, P.L., Ramette, A., 2014. A guide to statistical analysis in microbial ecology: a community-focused, living review of multivariate data analyses. FEMS Microbiol. Ecol. 90, 543–550.

Capo, E., Debroas, D., Arnaud, F., Guillemot, T., Bichet, V., Millet, L., Gauthier, E., Massa, C., Develle, A.L., Pignot, C., Lejzerowicz, F., Domaizon, I., 2016. Long-term dynamics in microbial eukaryotes communities: a paleolimnological view based on sedimentary DNA. Mol. Ecol. 25 (23), 5,925–5,943.

Capo, E., Debroas, D., Arnaud, F., Perga, M.E., Cècile, C., Domaizon, I., 2017. Tracking a century of changes in microbial eukaryotic diversity in lakes driven by nutrient enrichment and climate warming. Environ. Microbiol. 168 (3), 335–351.

Caron, D.A., Hutchins, D.A., 2013. The effects of changing climate on microzooplankton grazing and community structure: drivers, predictions and knowledge gaps. J. Plankton Res. 35 (2), 235–252.

Chen, X., Yang, X., Dong, X., Liu, Q., 2011. Nutrient dynamics linked to hydrological condition and anthropogenic nutrient loading in Chaohu Lake (southeast China). Hydrobiologia 661 (1), 223–234.

Chen, Y., Li, P., Huang, Y., Yu, K., Chen, H., Cui, K., Huang, Q., et al., 2019. Environmental media exert a bottleneck in driving the dynamics of antibiotic resistance genes in modern aquatic environment. Water Res. 162, 127–138.

Deng, D.G., Xie, P., Zhou, Q., Yang, H., Guo, L.G., 2007. Studies on temporal and spatial variations of phytoplankton in Lake Chaohu. J. of Integrated. Plant Biology. 49, 409–418.

Deshpande, B.N., Tremblay, R., Pienitz, R., Vincent, W.F., 2014. Sedimentary pigments as indicators of cyanobacterial dynamics in a hypereutrophic lake. J. Paleolimnol. 52 (3), 171–184.

Domaizon, I., Winegardner, A., Capo, E., Gauthier, J., Gregory-Eaves, I., 2017. DNA-based methods in paleolimnology: new opportunities for investigating long-term dynamics of lacustrine biodiversity. J. Paleolimnol. 58 (1), 1–21.

Dvořak, P., Casamatta, D.A., Poulickova, A., Hasler, P., Ondřej, V., Sanges, R., 2014. Synechococcus: 3 billion years of global dominance. Mol. Ecol. 23 (22), 5538–5551.

Ficetola, G.F., Poulenard, J., Sabatier, P., Messager, E., Gielly, L., Leloup, A., Etienne, D., Bakke, J., Malet, E., Fanget, B., Storen, E., Reyss, J.L., Taberlet, P., Arnaud, F., 2018. DNA from lake sediments reveals long-term ecosystem changes after a biological invasion. Sci. Adv. 4 (5), eaar4292.

Häder, D.P., Gao, K., 2014. Interactions of anthropogenic stress factors on phytoplankton. Frontiers in Environmental Science 3, 14.

Helbling, W.E., Banaszak, A.T., Villafañe, V.E., 2015. Global change feed-back inhibits cyanobacterial photosynthesis. Sci. Rep. 5 (1), 14514.

Huo, S., Li, X., Xi, B., Zhang, H., Ma, C., He, Z., 2020. Combining morphological and metabarcoding approaches reveals the freshwater eukaryotic phytoplankton community. Environmental Science Europe 32, 37.

Jiang, Y.J., He, W., Liu, W.X., Qin, N., Ouyang, H.L., Wang, Q.M., Kong, X.Z., He, Q.S., Yang, C., Yang, B., Xu, F.L., et al., 2014. The seasonal and spatial variations of phytoplankton community and their correlation with environmental factors in a large eutrophic Chinese lake (Lake Chaohu). Ecol. Indic. 40, 58–67.

Jiang, T., Yu, Z., Qi, Z., Chai, C., Qu, K., 2016. Effects of intensive mariculture on the sediment environment as revealed by phytoplankton pigments in a semi-enclosed bay, South China Sea. Aquac. Res. 48 (4), 1923–1935.

Karlsson, I.B., Sonnenborg, T.O., Refsgaard, J.C., Trolle, D., Borgesen, C.D., Olesen, J.E., et al., 2016. Combined effects of climate models, hydrological model structures and land use scenarios on hydrological impacts of climate change. J. Hydrol. 535, 301–317.

Komada, T., Anderson, M.R., Dorfmeier, C.L., 2008. Carbonate removal from coastal sediments for the determination of organic carbon and its isotopic signatures, $\delta^{13}C$ and $\delta\Delta^{14}C$: comparison of fumigation and direct acidification by hydrochloric acid. Limnology & Oceanography Methods 6 (6), 254–262.

Kosten, S., Huszar, V.L.M., Bécares, E., Costa, L.S., Donk, E.V., Hansson, L.A., Jeppesen, E., Kruk, C., Lacerot, G., Mazzeo, N., De Meester, L., Moss, B., Lurling, M., Noges, T., Romo, S., Scheffer, M., 2012. Warmer climates boost cyanobacterial dominance in shallow lakes. Glob. Chang. Biol. 18 (1), 118–126.

Li, F., Zhang, X., Xie, Y., Wang, J., 2019. Sedimentary DNA reveals over 150 years of ecosystem change by human activities in Lake Chao, China. Environ. Int. 133, 105214.

Maavara, T., Parsons, C.T., Ridenour, C., Stojanovic, S., Dürr, Hans H., Powley, H.R., Philippe, V.C., 2015. Global phosphorus retention by river damming. Proc. Natl. Acad. Sci. 112 (51), 15603–15608.

Maavara, T., Lauerwald, R., Regnier, P., Van Cappellen, P., 2017. Global perturbation of organic carbon cycling by river damming. Nat. Commun. 8 (1), 15347.

Mandakovic, D., Rojas, C., Maldonado, J., Latorre, M., Travisany, D., Delage, E., et al., 2018. Structure and co-occurrence patterns in microbial communities under acute environmental stress reveal ecological factors fostering resilience. Sci. Rep. 8 (1), 5875.

Mccabe, A.M., 1986. Glaciomarine facies deposited by retreating tidewater glaciers: an example from the late pleistocene of Northern Ireland. J. Sediment. Res. 56 (6), 880–894.

Michalak, A.M., Anderson, E.J., Beletsky, D., Boland, S., Bosch, N.S., 2016. Record-setting algal bloom in Lake Erie caused by agricultural and meteorological trends consistent with expected future conditions. Proc. Natl. Acad. Sci. 101 (16), 6,448–6,452.

Monchamp, M., Walser, J., Pomati, F., Spaak, P., 2016. Sedimentary DNA reveals Cyanobacterial community diversity over 200 years in two Perialpine Lakes. Appl. Environ. Microbiol. 82 (21), 6472–6482.

Monchamp, M., Spaak, P., Domaizon, I., Dubois, N., Bouffard, D., Pomati, F., 2018. Homogenization of lake cyanobacterial communities over a century of climate change and eutrophication. Nature Ecology and Evolution 2 (2), 317–324.

Mwangi, H.M., Julich, S., Patil, S.D., Mcdonald, M.A., Feger, K.H., 2016. Relative contribution of land use change and climate variability on discharge of upper Mara River, Kenya. J. of Hydrology Regional Studies 5 (1), 244–260.

Nübel, U., Garcia-Pichel, F., Muyzer, G., 1997. PCR primers to amplify 16S rRNA genes from Cyanobacteria. Appl. Environ. Microbiol. 63 (8), 3,327–3,332.

O'Beirne, M.D., Werne, J.P., Hecky, R.E., Johnson, T.C., Katsev, S., Reavie, E.D., 2017. Anthropogenic climate change has altered primary productivity in Lake Superior. Nat. Commun. 8, 15713.

O'Neil, J.M., Davis, T.W., Burford, M.A., Gobler, C.J., 2012. The rise of harmful cyanobacteria blooms: the potential roles of eutrophication and climate change. Harmful Algae 14, 313–334.

Paerl, H.W., Scott, J.T., Mccarthy, M.J., Newell, S.E., Gardner, W.S., Havens, K.E., Hoffman, D.K., Wilhelm, S.W., Wurtsbaugh, W.A., 2016. It takes two to tango: when and where dual nutrient (N & P) reductions are needed to protect lakes and downstream ecosystems. Environ. Sci. Technol. 50 (20), 10,805–10,813.

Paerl, H.W., Havens, K.E., Xu, H., Zhu, G.W., McCarthy, M.J., Newell, S.E., et al., 2019. Mitigating eutrophication and toxic cyanobacterial blooms in large lakes: the evolution of a dual nutrient (N and P) reduction paradigm. Hydrobiologia, (3) 1–17.

Pal, S., Gregoryeaves, I., Pick, F.R., 2015. Temporal trends in cyanobacteria revealed through DNA and pigment analyses of temperate lake sediment cores. J. Paleolimnol. 54 (1), 87–101.

Pearce, J.L., Beringer, J., Nicholls, N., Hyndman, R.J., Tapper, N.J., 2011. Quantifying the influence of local meteorology on air quality using generalized additive models. Atmos. Environ. 45 (6), 1328–1336.

Rigosi, A., Carey, C.C., Ibelings, B.W., Brookes, J.D., 2014. The interaction between climate warming and eutrophication to promote cyanobacteria is dependent on trophic state and varies among taxa. Limnol. Oceanogr. 59, 99–114.

Savichtcheva, O., Debroas, D., Perga, M.E., Arnaud, F., Villar, C., Lyautey, E., Kirkham, A., Chardon, C., Alric, B., Domaizon, I., 2015. Effects of nutrients and warming on *planktothrix* dynamics and diversity: a palaeolimnological view based on sedimentary DNA and RNA. Freshw. Biol. 60 (1), 31–49.

Smol, J.P., Wolfe, A.P., Birks, H.J., Douglas, M.S., Jones, V.J., Korhola, A., et al., 2005. Climate-driven regime shifts in the biological communities of arctic lakes. Proc. Natl. Acad. Sci. 102 (12), 4,397–4,402.

Spaak, J.W., Baert, J.M., Baird, D.J., Eisenhauer, N., Maltby, L., Pomati, F., Radchuk, V., Rohr, J.R., Van den Brink, P.J., De Laender, F., 2017. Shifts of community composition and population density substantially affect ecosystem function despite invariant richness. Ecol. Lett. 20 (10), 1315–1324.

Stager, J.C., Wiltse, B., Hubeny, J.B., Yankowsky, E., Nardelli, D., Primack, R., 2018. Climate variability and cultural eutrophication at Walden Pond (Massachusetts, USA) during the last 1800 years. PLoS One 13 (4), e0191755.

Su, W.G., Sha, Z.J., Kong, F.C., Yu, C.G., 2014. Sedimentary environment change in northwestern of Lake Qinghai based on the ^{137}Cs and ^{210}Pb. Acta Geol. Sin. 88, 27–28.

Thomas, M.K., Fontana, S., Reyes, M., Kehoe, M., Pomati, F., Coulson, T., 2018. The predictability of a lake phytoplankton community, over time-scales of hours to years. Ecol. Lett. 21, 619–628.

Tse, T.J., Doig, L.E., Leavitt, P.R., Quinones-Rivera, Z.J., Codling, G., Lucas, B.T., Liber, K., Giesy, J.P., Wheater, H., Jones, P.D., 2015. Long-term spatial trends in sedimentary algal pigments in a narrow river-valley reservoir, Lake Diefenbaker, Canada. J. Great Lakes Res. 41, 56–66.

Tse, T.J., Doig, L.E., Tang, S., Zhang, X., Sun, W., Wiseman, S.B., Feng, C.X., Liu, H., Giesy, J.P., Hecker, M., Jones, P.D., 2018. Combining high-throughput sequencing of *seda*DNA and traditional palaeolimnological techniques to infer historical trends in cyanobacterial communities. Environ. Sci. Technol. 52 (12), 6,842–6,853.

Wan, G.J., Santschi, P.H., Sturm, M., Farrenkothen, K., Lueck, A., Werth, E., Schuler, C., 1987. Natural (^{210}Pb, ^{7}Be) and fallout (^{137}Cs, $^{239,240}Pu$, ^{90}Sr) radionuclides as geochemical tracers of sedimentation in Greifensee, Switzerland. Chem. Geol. 63, 181–196.

Wan, G.J., Chen, J.A., Wu, F.C., Xu, S.Q., Bai, Z.G., Wan, E.Y., et al., 2005. Coupling between $^{210}Pb_{ex}$ and organic matter in sediments of anutrient-enriched lake: an example from Lake Chenghai, China. Chem. Geol. 224, 223–236.

Woolway, R.I., Kraemer, B.M., Lenters, J.D., Merchant, C.J., O'Reilly, C.M., Sharma, S., 2020. Global lake responses to climate change. Nature Reviews Earth & Environment https://doi.org/10.1038/s43017-020-0067-5.

Xue, B., Yao, S., Xia, W., Zhu, Y., 2010. Some sediment-geochemical evidence for the recent environmental changes of the lakes from the middle and lower Yangtze River basin, China. Quat. Int. 226, 29–37.

Yang, Z., Zhang, M., Shi, X., Kong, F., Ma, R., Yu, Y., 2016. Nutrient reduction magnifies the impact of extreme weather on cyanobacterial bloom formation in large shallow Lake Taihu (China). Water Res. 103, 302–310.

Yang, K., Yu, Z., Luo, Y., 2020. Analysis on driving factors of lake surface water temperature for major lakes in Yunnan-Guizhou plateau. Water Res. https://doi.org/10.1016/j.watres.2020.116018.

Zan, F., Huo, S., Xi, B., Su, J., Li, X., Zhang, J., Yeager, K.M., 2011. A 100 year sedimentary record of heavy metal pollution in a shallow eutrophic lake, Lake Chaohu, China. J. Environ. Monit. 13 (10), 2788–2797.

Zan, F., Huo, S., Xi, B., Zhu, C., Liao, H., Zhang, J., Yeager, K.M., 2012. A 100-year sedimentary record of natural and anthropogenic impacts on a shallow eutrophic lake, Lake Chaohu, China. J. of Environmental Monitoring 14 (3), 804–816.

Zapata, M., 2000. Separation of chlorophylls and carotenoids from marine phytoplankton: a new HPLC method using a reversed phase C8 column and pyridine-containing mobile phases. Mar. Ecol. Prog. Ser. 195 (3), 29–45.

Zeng, L., McGowan, S., Cao, Y., Chen, X., 2018. Effects of dam construction and increasing pollutants on the ecohydrological evolution of a shallow freshwater lake in the Yangtze floodplain. Sci. Total Environ. 621, 219–227.

Zhang, H., Huo, S., Yeager, K.M., He, Z., Xi, B., Li, X., Ma, C., Wu, F., 2019a. Phytoplankton response to climate changes and anthropogenic activities recorded by sedimentary pigments in a shallow eutrophied lake. Sci. Total Environ. 647, 1,398–1,409.

Zhang, C., Chang, H., Wang, H., Zhu, Y., Zhao, X., He, Y., Sun, F., Wu, F., 2019b. Spatial and temporal distributions of short-, medium-, and long chain chlorinated Paraffins in sediment cores from nine lakes in China. Environmental Science & Technology 53, 9462–9471.

Zhao, D., Shen, F., Zeng, J., Huang, R., Yu, Z., Wu, Q.L., 2016. Network analysis reveals seasonal variation of co-occurrence correlations between cyanobacteria and other bacterioplankton. Sci. Total Environ. 817–825.